The Journal of Experimental Biology 215, 2786-2794

doi:10.1242/jeb.071647

RESEARCH ARTICLE

Trafficking of bdelloid rotifer late embryogenesis abundant proteins

Rashmi Tripathi, Chiara Boschetti, Brian McGee† and Alan Tunnacliffe*

Cell and Organism Engineering Laboratory, Department of Chemical Engineering and Biotechnology, University of Cambridge, Cambridge CB2 3RA, UK

†Present address: GlaxoSmithKline, Stockley Park West, Uxbridge, Middlesex UB11 1BT, UK
*Author for correspondence (at10004@cam.ac.uk)

SUMMARY

The bdelloid rotifer *Adineta ricciae* is an asexual microinvertebrate that can survive desiccation by entering an ametabolic state known as anhydrobiosis. Two late embryogenesis abundant (LEA) proteins, ArLEA1A and ArLEA1B, have been hypothesized to contribute to desiccation tolerance in these organisms, since *in vitro* assays suggest that ArLEA1A and ArLEA1B stabilize desiccation-sensitive proteins and membranes, respectively. To examine their functions *in vivo*, it is important to analyse the cellular distribution of the bdelloid LEA proteins. Bioinformatics predicted their translocation into the endoplasmic reticulum (ER) *via* an N-terminal ER translocation signal and persistence in the same compartment *via* a variant C-terminal retention signal sequence ATEL. We assessed the localization of LEA proteins in bdelloids and in a mammalian cell model. The function of the N-terminal sequence of ArLEA1A and ArLEA1B in mediating ER translocation was verified, but our data showed that, unlike classical ER-retention signals, ATEL allows progression from the ER to the Golgi and limited secretion of the proteins into the extracellular medium. These results suggest that the N-terminal ER translocation signal and C-terminal ATEL sequence act together to regulate the distribution of rotifer LEA proteins within intracellular vesicular compartments, as well as the extracellular space. We speculate that this mechanism allows a small number of LEA proteins to offer protection to a large number of desiccation-sensitive molecules and structures both inside and outside cells in the bdelloid rotifer.

Supplementary material available online at: http://jeb.biologists.org/cgi/content/full/215/16/2786/DC1

Key words: anhydrobiosis, desiccation tolerance, late embryogenesis abundant protein, ER translocation signal, ER retention signal.

Received 23 February 2012; Accepted 4 April 2012

INTRODUCTION

Bdelloid rotifers are asexual, aquatic microinvertebrates with the ability to survive in environmental conditions where water is limiting, by losing most of their body water and entering a metabolically inert state. This phenomenon is known as anhydrobiosis (Ricci, 1998; Tunnacliffe and Lapinski, 2003). The molecular basis of their extreme biostability in this state remains largely elusive: unlike some other anhydrobiotic organisms that produce non-reducing disaccharides to counteract the effects of water loss, bdelloids lack such sugars (Lapinski and Tunnacliffe, 2003; Tunnacliffe and Lapinski, 2003; Caprioli et al., 2004; McGee, 2006). In the bdelloid *Adineta ricciae* (Segers and Shiel, 2005), a role in anhydrobiosis for two LEA proteins, ArLEA1A and ArLEA1B, has been proposed instead (Pouchkina-Stantcheva et al., 2007).

LEA proteins are a large family of proteins that were initially found to be produced in the later stages of embryo development in cotton seeds (Dure et al., 1981; Galau and Dure, 1981). Their expression was later also demonstrated in vegetative tissues of drought- and cold-stressed plants (Mundy and Chua, 1988; Joh et al., 1995). Moreover, they have been shown to be present in anhydrobiotic invertebrates including nematodes (Solomon et al., 2000; Browne et al., 2002), bdelloid rotifers (Tunnacliffe et al., 2005) and chironomids (Kikawada et al., 2006). Based on sequence similarity and amino acid composition, various classification schemes have been proposed for LEA proteins, the most common of which identifies three major groups (Dure et al., 1989; Tunnacliffe and Wise, 2007; Shih et al., 2008). Group 1 proteins are characterized by a hydrophilic 20-amino acid motif, group 2 proteins have at least two distinct sequence motifs and group 3 proteins contain multiple copies of an 11-amino acid motif, which has the potential to form α-helical structures on drying (Furuki et al., 2011).

ArLEA1A and ArLEA1B are group 3 LEA proteins encoded by the genes *Ar-lea-1A* and *Ar-lea-1B*, respectively, first identified in a cDNA population isolated from desiccating *A. ricciae* (Pouchkina-Stantcheva et al., 2007; Boschetti et al., 2011). Comparison of ArLEA1A and ArLEA1B protein sequences has revealed that they differ at only 12 of their matching amino acid positions. ArLEA1A is also longer due to an insert of an extra 44 amino acids. These subtle differences result in remarkably different biochemical properties of the two proteins (Pouchkina-Stantcheva et al., 2007): ArLEA1A behaves like the conventional nematode group 3 LEA protein, AavLEA1 (Goyal et al., 2003; Goyal et al., 2005b), being unstructured in solution, but acquiring α-helical structure on drying, and being able to reduce aggregation of desiccation-sensitive proteins. In contrast, ArLEA1B is unusual for a group 3 LEA protein in that it is partially structured, probably as a molten globule, in both the hydrated and dry states, and during drying it actually promotes aggregation of desiccation-sensitive enzymes; indeed, it aggregates itself. In addition, unlike ArLEA1A, ArLEA1B demonstrates a strong tendency to interact with dry liposomes (Pouchkina-Stantcheva et al., 2007). This feature is displayed by other LEA proteins, like LEAM and LEA7 (Tolleter et al., 2007;

Tolleter et al., 2010; Popova et al., 2011), which are thought to stabilize cellular membranes when water becomes scarce.

Despite this insight into the mode of action of ArLEA1A and ArLEA1B *in vitro*, our knowledge of their function in a cellular environment remains obscure. For example, it is not clear whether ArLEA1A and ArLEA1B might act in a specific subcellular location like LEAM, which localizes to plant mitochondria (Tolleter et al., 2007), or whether their effect might be more widely distributed within the cell. It is known (Pouchkina-Stantcheva et al., 2007) that ArLEA1A and ArLEA1B possess an N-terminal hydrophobic region and a C-terminal sequence ATEL that resembles endoplasmic reticulum (ER) retention signals like KDEL and HDEL (Munro and Pelham, 1987; Pelham, 1990), suggesting that ArLEA1A and ArLEA1B might be localized to the ER. We test this hypothesis by studying the intracellular localization of both full-length ArLEA1A and ArLEA1B tagged with the fluorescent protein mCherry, and of modified versions of both mCherry- and green fluorescent protein (GFP)-containing bdelloid LEA protein signal sequences. Our results suggest that ArLEA1A and ArLEA1B populate intracellular vesicular compartments, as well as the extracellular space.

MATERIALS AND METHODS

Bioinformatics

ArLEA1A, ArLEA1B and AavLEA1 protein sequences (accession numbers ABU62811.1, ABU62810.1 and AAL18843.1) were analysed using SignalP 4.0 (www.cbs.dtu.dk/services/SignalP) and TargetP 1.1 (www.cbs.dtu.dk/services/TargetP).

Rotifers, antibodies and immunoblotting

The bdelloid rotifer (*A. ricciae*) clone AR6.3 was grown and collected as described (Pouchkina-Stantcheva and Tunnacliffe, 2005), except that animals were detached from culture vessel surfaces by vigorous shaking. Polyclonal antibodies were derived from sera of rabbits immunized with recombinant ArLEA1A (Pouchkina-Stantcheva et al., 2007) according to a standard 80-day protocol (Harlan Sera-Labs, Loughborough, UK). Affinity purification of antibodies from crude serum was performed as described (Goyal et al., 2003) using recombinant ArLEA1A cross-linked to an Affigel-10 (Bio-Rad, Hemel Hempstead, UK) column. Immunoblotting methods for invertebrate and mammalian cell extracts have been described (Goyal et al., 2003; Chakrabortee et al., 2010). Primary antibody against ArLEA1A was used at 1:10,000 dilution, and secondary antibody at 1:4000 dilution.

Confocal microscopy

Adult rotifers were collected as described (Pouchkina-Stantcheva and Tunnacliffe, 2005) and resuspended in water; 15 µl rotifer suspension was pipetted onto a poly-lysinated slide and overlaid with a coverslip. The slide was immediately immersed in liquid N_2 for 10 s, then the coverslip removed to freeze-crack the rotifers. Slides were incubated in 4% paraformaldehyde in PBS (110 mmol l^{-1}, pH 7.4) at room temperature for 20 min on an orbital shaker. Slides were washed three times for 5 min in PBS, incubated for 30 min in 0.5% Triton X-100 and 0.25% Tween-20, then washed once for 5 min in PBST (PBS plus 0.2% Tween-20). The slides were then blocked for 30 min in PBST containing 1% BSA in a humidity chamber. Animals were incubated in a 1:100 dilution of anti-AriLEA1A antibody in PBST at 4°C overnight in a humidity chamber, then washed three times in PBST. Slides were blocked again in PBST with 1% BSA for 30 min, incubated for 30 min in 0.5% Triton X-100 and 0.25% Tween-20, then washed three times for 5 min in PBST. Slides were incubated with preabsorbed anti-rabbit Cy3-linked antibody (Thermo Scientific, Rockford, IL, USA) at a dilution of 1:100 in PBST for 30 min at 4°C in a dark humidity chamber. Slides were washed three times for 5 min in PBS and then mounted with antifade mounting medium containing DAPI, and sealed with nail polish. Imaging was performed using a Zeiss LSM 510 META laser scanning confocal microscope (X63, 1.4 N.A., Plan apochromat objective). Excitation wavelengths were 405 nm for DAPI, 488 nm for GFP and 543 nm for Cy3/mCherry; emission wavelengths were 420–480 nm for DAPI, 505–530 nm for GFP/EGFP and 560–615 nm for mCherry/Cy3. For the co-localization analysis in mammalian cells, the voxel dimensions were set according to the Nyquist criteria (Scriven et al., 2008). The x, y and z dimensions of pixel sizes were calculated according to the shorter wavelength (488 nm) as x=43 nm; y=43 nm; z=0.13 µm; digital zoom: 1.6; resolution: 2048; pinhole size: 1 Airy unit. Calculations were made using www.svi.nl/NyquistCalculator. Images were processed using manufacturer's software. 2-D pixel analysis of red and green channel intensities was performed using JACoP (Just Another Colocalisation Plug-in) (Bolte and Cordelières, 2006) in ImageJ 1.45s.

Recombinant DNA methods

ArLEA1A and ArLEA1B were PCR amplified using NotI-digested cDNA clones (Pouchkina-Stantcheva et al., 2007) with Phusion high-fidelity DNA Polymerase (Thermo Scientific). KpnI and NheI restriction sites were engineered at the 5′ end, while a sequence encoding a FLAG tag and a BamHI restriction site were engineered at the 3′ end of PCR products. ArLEA1A and ArLEA1B were cloned into pcDNA3.0-mCherry (obtained from Dr Sohini Chakrabortee) using the KpnI and BamHI restriction sites in frame with the mCherry gene (ArLEA1A/1B-FLAG-mCherry constructs). mCherry and EGFP proteins containing an N-terminal signal peptide sequence and C-terminal ATEL, KDEL or 'ochre' stop codon sequences were PCR amplified from linearized pcDNA3.0-mCherry and pET-28a-EGFPHDQ74 (obtained from Oliver Wright), respectively, and cloned into pcDNA3.3 TOPO vector (Invitrogen, Paisley, UK). All inserts were verified by DNA sequencing. Supplementary material Fig. S1 shows a diagrammatic representation of all the constructs.

CterGMAP210GFP and NterGMAP210GFP constructs

GMAP210 is a long coiled-coil *cis*-Golgi-associated protein that plays a role in maintaining Golgi ribbon integrity and position (Yadav et al., 2009). The N-terminal end of GMAP210 fused to GFP (NterGMAP210GFP) has been found to concentrate in vesicles lying in the periphery of Golgi elements, while the C-terminal end of GMAP210 fused to GFP (CterGMAP210GFP) appears to be distributed uniformly in the *cis*-cisternae of the Golgi apparatus (Cardenas et al., 2009). CterGMAP210 and NterGMAP210 constructs cloned in pGFP-N and pGFP-C vectors were obtained from Jesús Cárdenas from CABIMER-CSIC, Seville, Spain, and used as Golgi markers.

Cell culture and transfections

Mammalian COS-7 cells were grown in Dulbecco's modified Eagle's medium (DMEM, Sigma-Aldrich, Poole, UK) supplemented with 10% FBS (Sigma), 1% L-glutamine–penicillin–streptomycin solution (Sigma) in a humidified 5% CO_2 atmosphere at 37°C. Transient transfection was performed using GeneJammer Transfection reagent (Agilent Technologies, Wokingham, UK) according to the manufacturer's instructions. For colocalization analysis, COS-7 cells were allowed to reach 70–80% confluence in 35 mm MatTek glass bottom plates. Plasmid DNA (0.75/1 µg) was

used for single/double transfections with 4.5/6.0 µl of GeneJammer transfection reagent, respectively. Cells were visualized by confocal microscopy after 24 h. For supernatant analysis, COS-7 cells were grown on 10 cm diameter dishes (Nunc, Thermo Scientific), until they reached 70–80% confluence, then transfected with 3 µg of DNA. Twelve hours post-transfection, medium was changed to DMEM (without FBS). Supernatants were harvested after overnight incubation. To confirm expression of ArLEA1A-FLAG-mCherry and ArLEA1B-FLAG-mCherry by western blot, 1 µg each of pcDNA3.0-ArLEA1A-FLAG-mCherry, pcDNA3.0-ArLEA1B-FLAG-mCherry, pcDNA3.0-AavLEA1-FLAG-mCherry and pcDNA3.0-mCherry plasmids were transfected in COS-7 cells growing on 6-well plates (Nunc), using 6.0 µl GeneJammer. Cells were harvested 48 h post-transfection.

ER-Tracker Green and MitoTracker Green staining

ER-Tracker Green (BODIPY FL glibenclamide) (Invitrogen) stock solution (prepared in DMSO) was diluted to 1 µmol l^{-1} in pre-warmed Hanks' balanced salt solution (HBSS). After removing media, cells were rinsed with HBSS and prewarmed staining solution was added, then incubated at 37°C for 30 min. The staining solution was subsequently removed and prewarmed PBS with 2% FBS was added to view cells under the confocal microscope. For MitoTracker Green FM (Invitrogen) staining, stock solution (prepared in DMSO) was diluted to 100 nmol l^{-1} in prewarmed DMEM. The growth medium was replaced with 2 ml staining medium and cells were incubated at 37°C for 15 min. The staining medium was subsequently replaced with prewarmed media and cells were visualized under the confocal microscope.

mCherry fluorescence measurements

Supernatants obtained after transfection experiments were centrifuged at 3540 ***g*** and 4°C to pellet cell debris. Vivaspin 2 concentrators (Sartorius Stedim, Epsom, UK) were used to concentrate supernatants following the manufacturer's instructions. Supernatants (4 ml) were concentrated to approximately 200 µl. Protein concentration of supernatants was determined using a DC Protein Assay kit (Bio-Rad). Fluorescence measurements were carried out using a normalized amount of protein in all samples, with an EnVision plate reader (PerkinElmer, Cambridge, UK) in a 96-well opaque OptiPlate, using an excitation wavelength of 544 nm. Emitted light was collected at 615 nm. The number of flashes was set to 10.

Statistical analysis

All statistical analysis was performed using the InStats package version 3.1a (GraphPad Software, La Jolla, CA, USA). As the fluorescence values did not pass the Kolmogorov–Smirnov (KS) normality test, square-root transformation of the data was performed. Statistical significance between different groups was determined by one-way ANOVA and Tukey's *post hoc* test. Data were plotted using Microsoft Excel.

RESULTS

Bioinformatics predictions for ArLEA1A and ArLEA1B localization

The N-terminal signal sequence of proteins usually consists of hydrophobic amino acids that enable the cotranslational translocation of a newly synthesized polypeptide chain across the phospholipid bilayer of the ER (High, 1995). To identify the signal sequences in ArLEA1A and ArLEA1B, we used SignalP 4.0, which distinguishes between signal peptides and N-terminal transmembrane helices (Petersen et al., 2011). The most significant signal peptidase cleavage site is predicted between amino acid positions 19 and 20 in both ArLEA1A and ArLEA1B (supplementary material Fig. S2A,B) with a maximum S-score (signal sequence prediction score) of 0.95 and a C-score (cleavage site prediction score) of 0.695 due to sequence identity in their N-terminal region. In contrast, AavLEA1, derived from anhydrobiotic nematode *Aphelenchus avenae*, lacks any N-terminal signal sequences or cleavage site, as indicated by low S- and C-scores (supplementary material Fig. S2C). TargetP 1.1 (Emanuelsson et al., 2007) is another tool for subcellular localization predictions of newly synthesized proteins. Using the N-terminal sequence information, it discriminates between proteins destined for the mitochondrion, the chloroplast (for plant sequences) or the secretory pathway. Both ArLEA1A and ArLEA1B show high scores (0.95) for localization in the secretory pathway and correspondingly low scores for mitochondrial targeting (0.029). AavLEA1, on the other hand, gives a very low score for localization in the secretory pathway and mitochondria (0.043 and 0.156, respectively). Hence both SignalP and TargetP indicate a high probability of translocation of ArLEA1A and ArLEA1B into the ER *via* N-terminal signal sequences.

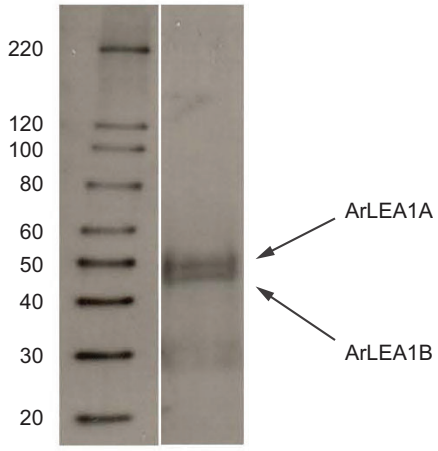

Fig. 1. Immunoblot of *Adineta ricciae* protein extracts with polyclonal antibodies raised against ArLEA1A. Proteins were separated on a 12% SDS-polyacrylamide gel. The left-hand lane shows mass standards in kDa. Approximately 20 µg bdelloid protein was run in the right-hand lane.

ArLEA1A and ArLEA1B in bdelloid rotifers

To attempt to localize the LEA proteins within bdelloids, a polyclonal antiserum was first raised against recombinant ArLEA1A, and the resulting antibodies were affinity purified against the same protein. The polyclonal antibodies recognized recombinant forms of both ArLEA1A and ArLEA1B (McGee, 2006), as anticipated since they have very similar sequences (Pouchkina-Stantcheva et al., 2007), and in immunoblotting experiments with protein extracts of *A. ricciae*, two bands of approximately the expected mass were detected (Fig. 1). ArLEA1A and ArLEA1B have predicted masses of 44.5 and 39.8 kDa, respectively, and if the predicted signal peptides are cleaved, these become 42.5 and 37.8 kDa, respectively. Both proteins migrate slightly higher than expected, as do other LEA proteins (Tunnacliffe and Wise, 2007), probably due to incomplete binding of sodium dodecyl sulphate (SDS). A faint signal was also detected at around 30 kDa, indicating either the presence of other smaller LEA proteins

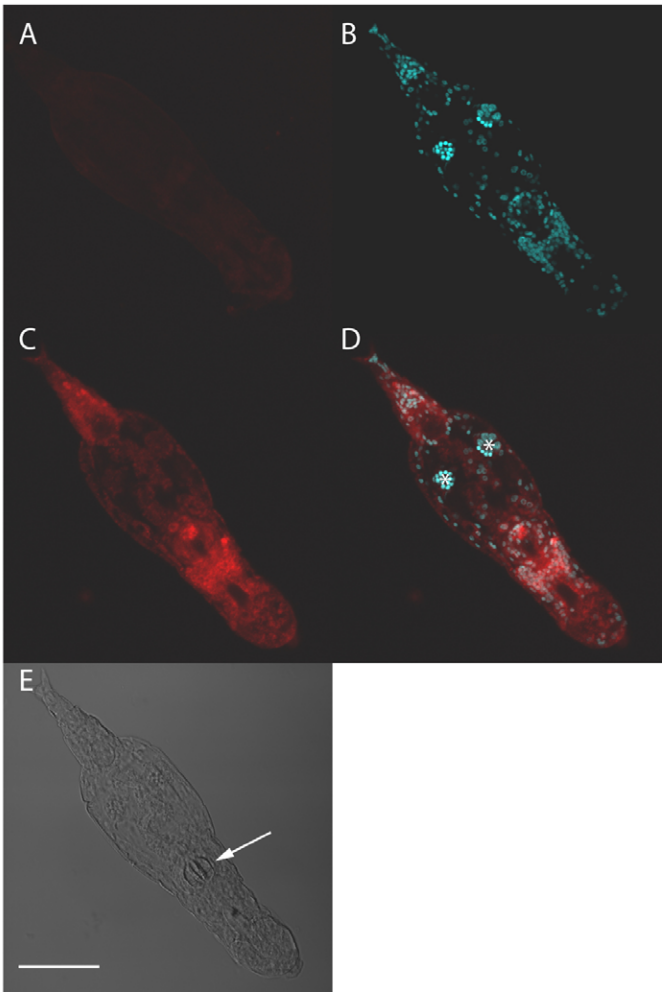

Fig. 2. Indirect immunostaining of LEA proteins in *A. ricciae* in hydrated animals. (A) Specimen treated without primary antibody as a control; (B–E) a specimen treated with both primary and secondary antibodies to show LEA proteins. (B) DAPI (blue) staining to highlight nuclei; (C) LEA proteins staining (red); (D) composite image of (B) and (C); (E) transmitted light of the same animal. The vitellaria are indicated by asterisks. The arrow indicates the mastax, shown at higher magnification in supplementary material Fig. S3. Scale bar, 30 μm.

or processing of ArLEA1A and ArLEA1B into smaller peptides (Goyal et al., 2005a; Kikawada et al., 2006).

To determine the location of ArLEA1A and ArLEA1B within the bdelloid, immunostaining was performed using the purified ArLEA1A antibodies and images were obtained by confocal microscopy. The LEA proteins were seen to be present throughout the whole length of the hydrated animal, and were particularly prominent in those areas with densely packed cells (shown by blue DAPI counterstaining of the nuclei), with the exception of the vitellarium (Fig. 2). At higher magnification, for example in the region around the mastax, it was shown that LEA protein staining was absent from nuclei, and present in the cytoplasmic space, but it was difficult to localize the signal further (supplementary material Fig. S3).

ArLEA1A and ArLEA1B translocate into the ER

Since rotifer cell cultures are not available, intracellular LEA protein localization was assessed after expression of tagged proteins in mammalian cells. COS-7 cells were transfected with pcDNA3.0 containing ArLEA1A-FLAG-mCherry, ArLEA1B-FLAG-mCherry or mCherry (supplementary material Fig. S1), and expression of ArLEA1A and ArLEA1B fusion proteins was verified by immunoblotting (supplementary material Fig. S4). As can be observed, both ArLEA1A-FLAG-mCherry and ArLEA1B-FLAG-mCherry migrate higher than expected in a manner similar to native ArLEA1A and ArLEA1B in *A. ricciae*.

Cells expressing ArLEA1A-FLAG-mCherry, ArLEA1B-FLAG-mCherry and mCherry were stained with ER-Tracker Green (BODIPY FL glibenclamide; Invitrogen), a cell-permeant, live-cell stain that binds to sulfonylurea receptors of ATP-sensitive K^+ channels in the ER membrane, and colocalization was assessed by confocal microscopy. Images obtained within the red and green channels were merged and the fluorescent intensity signals were measured in selected regions (Fig. 3A–C). For cells containing ArLEA1A-FLAG-mCherry and ArLEA1B-FLAG-mCherry, overlap of the red and green fluorescence signals was observed, indicating colocalization with ER-Tracker Green. This overlap is not complete, however, possibly due to the delivery of ArLEA1A and ArLEA1B to vesicles and compartments outside the ER. In contrast, mCherry alone is mostly distributed both in the cytoplasm and in the nucleus (Fig. 3C; and data not shown). Some mCherry is observed to colocalize with ER-Tracker Green, possibly due to its hydrophobic residues that might favour its association with the ER membrane. Higher magnification might enable better resolution of the two compartments. As a control, ArLEA1A-FLAG-mCherry and ArLEA1B-FLAG-mCherry signal location was compared with that of MitoTracker Green, a mitochondrial stain. Fig. 3D,E shows no overlap between the red and green channels.

A 2D scatter plot analysis of colocalized pixel intensites for the red and green channels confirmed the above conclusions (supplementary material Fig. S5): both ArLEA1A-FLAG-mCherry and ArLEA1B-FLAG-mCherry show higher Pearson's and Mander's correlation values with ER-Tracker Green (0.37, 0.72, 0.44 and 0.62, 0.90, 0.65, respectively) than mCherry (0.14, 0.07, 0.49). In contrast, ArLEA1A-FLAG-mCherry and ArLEA1B-FLAG-mCherry show low Pearson's and Mander's correlation values with MitoTracker Green (–0.03, 0.02, 0.09 and –0.02, 0.09, 0.13, respectively). These results demonstrate the translocation of ArLEA1A and ArLEA1B into the ER and corroborate the bioinformatics predictions for ER translocation of these proteins.

ATEL and KDEL retention signals mediate differential localization within the secretory pathway

The ArLEA1A-FLAG-mCherry and ArLEA1B-FLAG-mCherry fusion proteins cannot be used to test the function of the putative ER retention signal ATEL since such signals are masked if not positioned at the C-terminus (Pelham, 1990). Therefore, a new set of plasmids was made where the DNA sequence corresponding to the first 22 amino acids of ArLEA1A and ArLEA1B (termed 'NS') was cloned in frame with mCherry at the 5′ end, and either the rotifer sequence ATEL or the conventional ER retention signal KDEL were engineered at the 3′ end. NS-mCherry without a C-terminal signal was also produced as a control. COS-7 cells transfected with either NS-mCherry, NS-mCherry-KDEL or NS-mCherry-ATEL and stained with ER-Tracker Green showed that NS-mCherry-KDEL colocalized substantially with ER-Tracker Green (supplementary material Fig. S6A), but either ATEL or stop codon at the C-terminus resulted in only partial overlap of red and green signals, suggesting the presence of mCherry in compartments

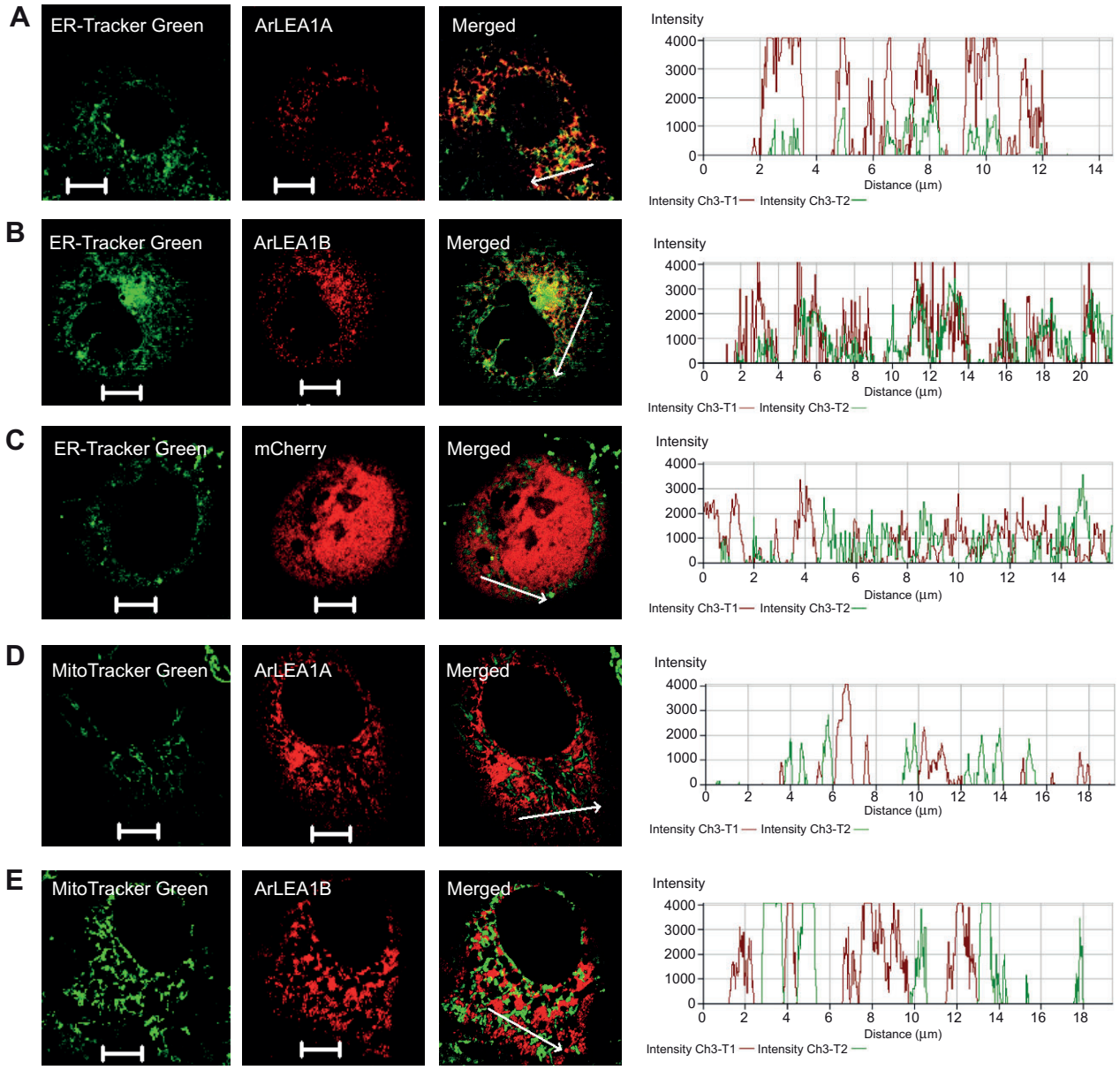

Fig. 3. Translocation of ArLEA1A and ArLEA1B into the ER. COS-7 cells were transfected with pcDNA3.0 vector containing mCherry-tagged ArLEA1A and ArLEA1B, and 24 h post-transfection cells were stained with ER-Tracker Green or MitoTracker Green at 37°C. Live-cell imaging was performed with a confocal microscope. Colocalization is observed between ER-Tracker Green and (A) ArLEA1A and (B) ArLEA1B. (C) mCherry is mostly cytoplasmic and nuclear in distribution. No colocalization is observed between MitoTracker Green and (D) ArLEA1A and (E) ArLEA1B. Left, green channel (GFP); middle, red channel (mCherry); right, red/green merged image; far right, plot showing red and green fluorescent intensities, indicated by Ch3-T1 and Ch3-T2, respectively, at selected region of interest (arrows in the far right merged image). Scale bars, 10 μm.

other than the ER (supplementary material Fig. S6B,C). Supplementary material Fig. S5 shows the 2D scatter plot of colocalized pixel intensities for the red and green channels and the corresponding correlation values. NS-mCherry-KDEL shows higher Pearson's and Mander's correlation values with ER-Tracker Green (0.5, 0.6, 1.0) compared with NS-mCherry-ATEL (0.3, 0.5, 0.5) and NS-mCherry (0.3, 0.3, 0.6).

To examine this further, we produced constructs with EGFP containing an N-terminal signal and either KDEL or ATEL at the C-terminal end (supplementary material Fig. S1). COS-7 cells were then cotransfected with either NS-mCherry-ATEL or NS-mCherry-KDEL, and either NS-EGFP-ATEL or NS-EGFP-KDEL. As shown in Fig. 4A,B, the red and green channel intensities show good overlap when cells are cotransfected with NS-mCherry-KDEL and NS-EGFP-KDEL or NS-mCherry-ATEL and NS-EGFP-ATEL. However, NS-EGFP-ATEL and NS-mCherry-ATEL seem to only partially colocalize with NS-mCherry-KDEL and NS-EGFP-KDEL, respectively (Fig. 4C,D). The 2D scatter plots for colocalization between red and green channels confirm this interpretation, with Pearson's and Mander's correlation values for cotransfection of NS-mCherry-KDEL and NS-EGFP-KDEL of 0.87, 0.95 and 0.91; for NS-mCherry-ATEL and NS-EGFP-ATEL of 0.76, 0.82 and 0.92; for NS-mCherry-KDEL and NS-EGFP-ATEL of 0.43, 0.79 and 0.54; and for NS-mCherry-ATEL and NS-EGFP-KDEL of 0.50,

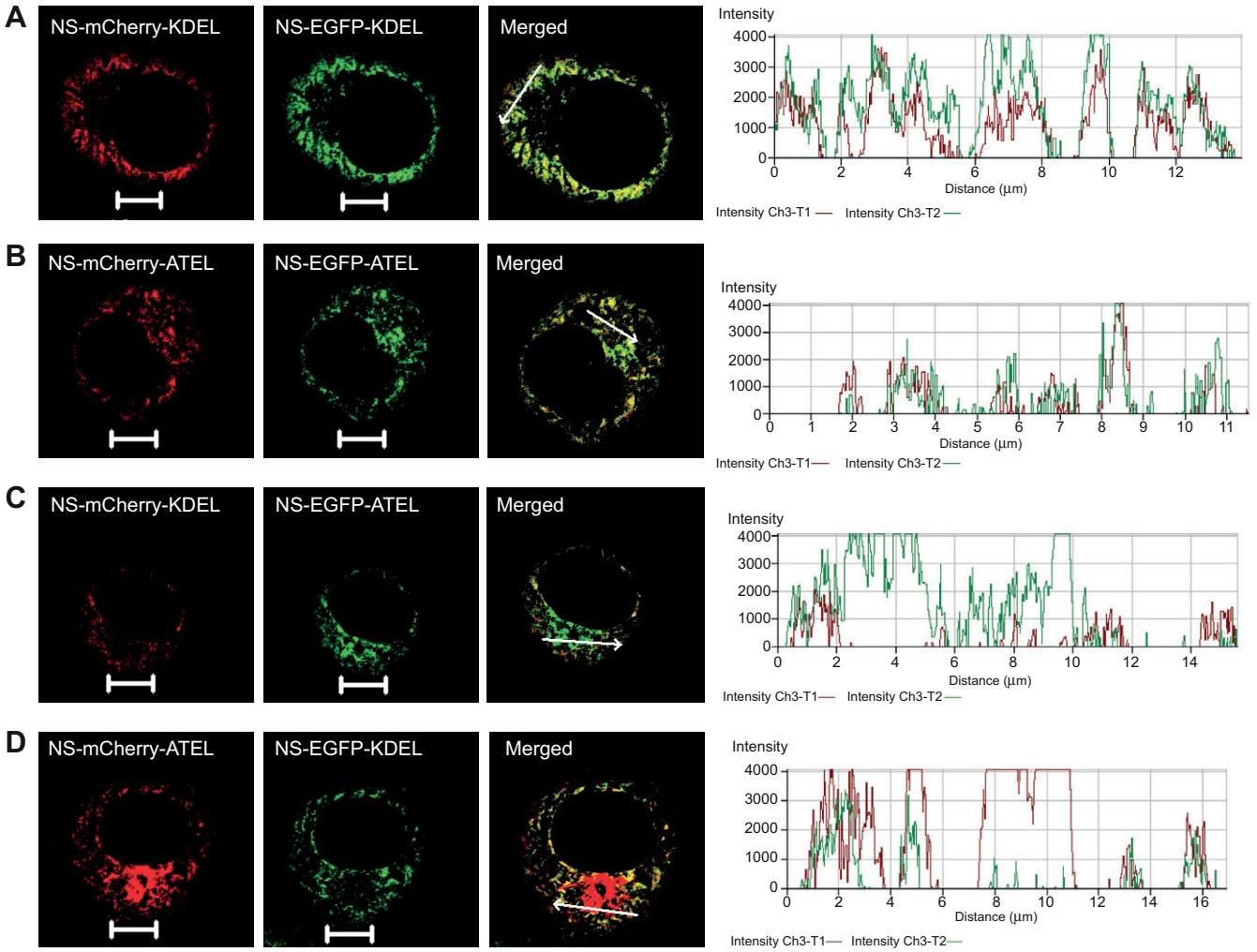

Fig. 4. ATEL and KDEL sequences mediate differential localization. COS-7 cells were cotransfected with pcDNA3.3 containing the following constructs: (A) NS-mCherry-KDEL and NS-EGFP-KDEL; (B) NS-mCherry-ATEL and NS-EGFP-ATEL; (C) NS-mCherry-KDEL and NS-EGFP-ATEL and (D) NS-mCherry-ATEL and NS-EGFP-KDEL. Cells were observed under the confocal microscope, 24 h post-transfection. Similar localization patterns for red and green channels are observed when NS-EGFP and NS-mCherry contain identical C-terminal sequences (A,B). However, different localization patterns are observed when cells are cotransfected with constructs containing non-identical C-terminal sequences (C,D). Left, green channel (EGFP); middle, red channel (mCherry); right, red/green merged image; far right, plot showing red and green fluorescent intensities, indicated by Ch3-T1 and Ch3-T2, respectively, in the selected region of interest (arrows in the far right merged image). Scale bars, 10 µm.

0.51 and 0.91 (data not shown). Compartments enriched for ATEL-tagged mCherry or EGFP seem to lie close to the nucleus in a pattern reminiscent of the Golgi apparatus.

ATEL, but not KDEL, colocalizes with Golgi stacks and vesicles

To confirm the presence of ATEL-tagged proteins in the Golgi, colocalization analysis of NS-mCherry-KDEL or NS-mCherry-ATEL with GFP-tagged GMAP210 constructs was performed. The N-terminal end of GMAP210 fused to GFP (NterGMAP210GFP) has been found to concentrate in vesicles lying in the periphery of Golgi elements, while the C-terminal end of GMAP210 fused to GFP (CterGMAP210GFP) appears to be distributed uniformly in the *cis*-cisternae of the Golgi apparatus (Cardenas et al., 2009). There seems to be poor colocalization of NS-mCherry-KDEL with either NterGMAP210GFP or CterGMAP210GFP (Fig. 5A,B), while NS-mCherry-ATEL is found to overlap partially with both NterGMAP210GFP and CterGMAP210GFP (Fig. 5C,D). The corresponding scatter plots of colocalized pixel intensities and correlation values are 0.08, 0.05 and 0.53 for NS-mCherry-KDEL and CterGMAP210GFP; 0.01, 0.00 and 0.23 for NS-mCherry-KDEL and NterGMAP210GFP; 0.47, 0.33 and 0.94 for NS-mCherry-ATEL and CterGMAP210GFP; and 0.19, 0.08 and 0.84 for NS-mCherry-ATEL and NterGMAP210GFP.

ATEL regulates secretion into the extracellular medium

The fact that ATEL-containing proteins are present in both ER and Golgi raises the question of whether ATEL has any retention function at all; if not, we might expect ATEL-containing proteins to progress to the extracellular space to a similar extent as those without ATEL. Therefore, mCherry fluorescence was measured in supernatants of COS-7 cells expressing mCherry, NS-mCherry, NS-mCherry-KDEL or NS-mCherry-ATEL. Untransfected cells were used as controls. The means and standard deviations (N=3) were plotted (Fig. 6). One-way ANOVA showed that statistical difference between various groups was highly significant ($F_{4,10}$=1671.5,

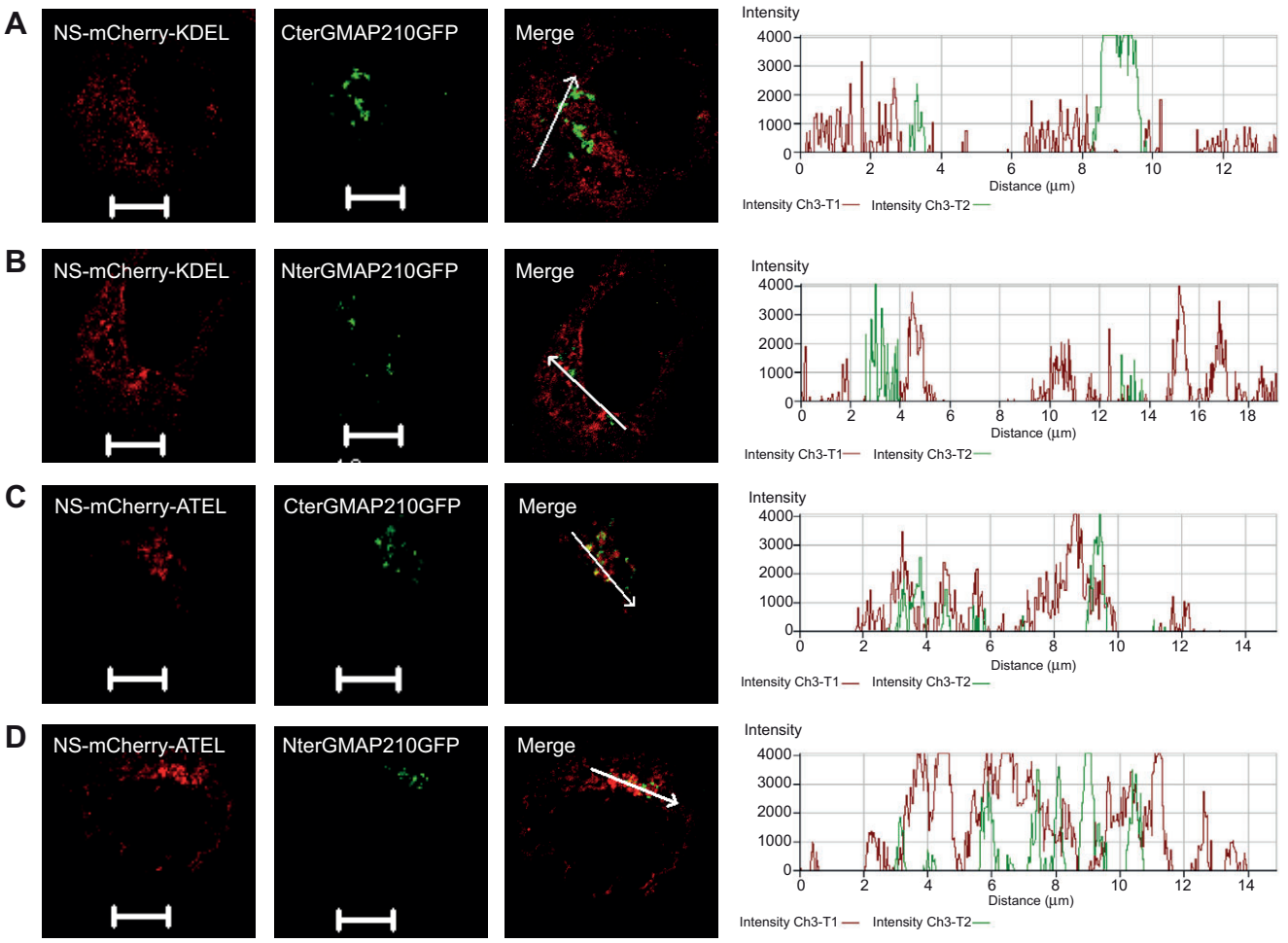

Fig. 5. ATEL allows progression into Golgi. COS-7 cells were cotransfected with NS-mCherry-KDEL or NS-mCherry-ATEL and GFPCterGMAP210 or NterGMAP210GFP constructs. Cells were observed 24 h post-transfection. Scant colocalization is observed between NS-mCherry-KDEL and (A) CterGMAP210GFP or (B) NterGMAP210GFP. In contrast, NS-mCherry-ATEL is observed to partially colocalize with both (C) CterGMA210GFP and (D) NterGMAP210GFP. Left, red channel (mCherry); middle, green channel (GFP); right, red/green merged image; far right, plot showing red and green fluorescent intensities, indicated by Ch3-T1 and Ch3-T2, respectively, in the selected region of interest (arrows in the far right merged image). Scale bars, 10 μm.

P<0.0001). Pair-wise comparison between different groups performed using Tukey's *post-hoc* test revealed that mCherry fluorescence was significantly enhanced (P<0.001) in supernatants of cells expressing NS-mCherry compared with other experimental groups, suggesting efficient secretion of NS-mCherry to the cell exterior. The fluorescence values of both NS-mCherry-KDEL and NS-mCherry-ATEL were significantly reduced compared with cells expressing NS-mCherry (P<0.001). However, secretion of NS-mCherry-ATEL was significantly higher (P<0.001) than NS-mCherry-KDEL. These results suggest that although both ATEL and KDEL mediate retention of mCherry within the secretory pathway, ATEL allows more leakage to the cell exterior and is not as effective as KDEL in retaining proteins within the ER.

DISCUSSION

Unlike most life forms that cannot survive in the absence of water, bdelloid rotifers are able to undergo anhydrobiosis. The molecular basis of their extreme biostability in this state is still unclear. Recently, two proteins, ArLEA1A and ArLEA1B, belonging to the LEA protein family, were identified in the desiccation-induced gene set in bdelloid rotifers (Pouchkina-Stantcheva et al., 2007). However, our results in this paper show that these proteins are also found in hydrated animals. These results might imply that the presence of LEA proteins prepares the bdelloids for water stress before it happens, thus enabling them to quickly adapt to it when it occurs.

Previous work on the functional characterization of ArLEA1A and ArLEA1B suggested a role in preventing protein aggregation and in stabilizing membranes, respectively (Pouchkina-Stantcheva et al., 2007). It was speculated that these functions operated after translocation into, and possibly retention in, the ER. While it is technically difficult to test these predictions in bdelloids themselves, use of a mammalian cell model has allowed confirmation of the function of the N-terminal signal peptide sequences of ArLEA1A and ArLEA1B, and assessment of a putative C-terminal ER retention signal, ATEL.

Proteins normally enter the ER cotranslationally and are either retained there or targeted to other destinations including the Golgi (Bannykh et al., 1998), lysosomes (Andrews, 2000) or the cell exterior (Burgess and Kelly, 1987). Their functions within the ER might include lipid biosynthesis (Sisson and Fahrenbach, 1967;

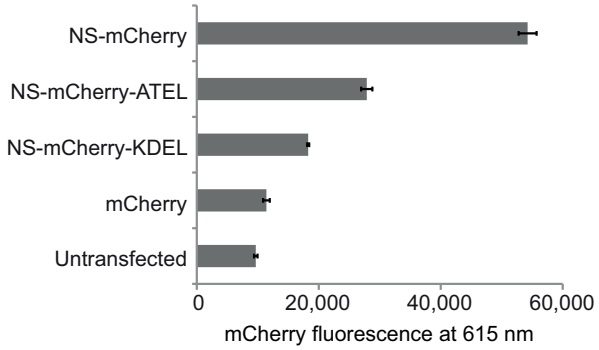

Fig. 6. ATEL retards secretion into extracellular medium. mCherry fluorescence was measured in concentrated (20×) supernatants of COS-7 cells expressing NS-mCherry, NS-mCherry-ATEL, NS-mCherry-KDEL and mCherry, 24 h post-transfection. Untransfected cells were used as controls. Measurements were made using a Perkin-Elmer plate-reader at 615 nm. The mean and standard deviation are plotted.

Black, 1972), participation in 'quality control' processes of other proteins and lipids (Hammond and Helenius, 1995), mediating the unfolded protein response within the ER (Chakrabarti et al., 2011), calcium storage (Martone et al., 1993; Sammels et al., 2010) and secretion (Wiest et al., 1990). Protein retention within the ER is most commonly signal dependent, controlled by sequence-specific receptors (Munro and Pelham, 1987; Pelham, 1990).

It is known that the C-terminal sequence KDEL (or its variants) retains soluble proteins within the ER by retrograde transport from the early Golgi compartments by binding to KDEL receptors (Wilson et al., 1993) and trafficking them back to the ER *via* COPI-coated vesicles (Letourneur et al., 1994). However, it has also been shown that this system allows some leakage of ER-resident proteins into the extracellular medium, as observed for phytohemaglutinin in plant cells (Herman et al., 1990) and protein disulfide isomerase in a rat pancreatic exocrine cell line (Yoshimori et al., 1990). Hence our finding that a small amount of KDEL-tagged protein is detected in the supernatants is not surprising. Additionally, our results suggest that proteins containing ATEL are retained to a limited degree within the ER, and that unlike KDEL, greater population of other compartments of the secretory system, and indeed the extracellular space, also occurs. This is consistent with a study that examined the ER retention capacity of 152 variants of KDEL in mammalian cells (Raykhel et al., 2007). Unfortunately, the authors did not include ATEL in their panel of variants, but they showed that the –3 position (i.e. T in ATEL) is not particularly important (unless it is proline). Therefore, ATEL is probably similar in function to ADEL, for example, which was shown to allow at least 50% of associated protein to escape the ER.

Although extrapolating results from a mammalian cell to an invertebrate requires caution, trafficking mechanisms are highly conserved between yeast and humans (Dancourt and Barlowe, 2010), so it is possible that ArLEA1A and ArLEA1B are present throughout intracellular vesicular compartments, as well as in the extracellular tissue fluid, in the bdelloid. This would allow a small number of protective proteins to police a large physiological space in the animal, consistent with a role in stress tolerance. In higher eukaryotes, extracellular chaperones have recently attracted attention, with proteins such as clusterin and apolipoprotein E thought to monitor aggregating peptides implicated in Alzheimer's disease, for example (Wilson et al., 2008). As denaturation and aggregation is likely to be a risk for extracellular as well as intracellular proteins subjected to desiccation, multicellular organisms that undergo anhydrobiosis are likely to have similar protection mechanisms operating outside cells. ArLEA1A and ArLEA1B might therefore form part of such extracellular surveillance mechanisms.

LIST OF ABBREVIATIONS

LEA	late embryogenesis abundant
GFP	green fluorescent protein
EGFP	enhanced GFP
PBS	phosphate-buffered saline
BSA	bovine serum albumin
DAPI	4′,6-diamidino-2-phenylindole
FBS	fetal bovine serum
DMSO	dimethyl sulfoxide

ACKNOWLEDGEMENTS

We would like to thank Jesús Cárdenas for GMAP210 constructs, Sohini Chakrabortee for suggestions on designing the bdelloid LEA–mCherry fusion constructs, and David Macherel for advice on live-cell imaging with mitochondrial stains.

FUNDING

This study was funded by the European Research Council (Advanced Investigator Grant 233232) and the Biotechnology and Biological Sciences Research Council (grants BB/F020856/1 and 02/A2/P/08059). R.T. was also supported by Cambridge Commonwealth Trust.

REFERENCES

Andrews, N. W. (2000). Regulated secretion of conventional lysosomes. *Trends Cell Biol.* **10**, 316-321.
Bannykh, S. I., Nishimura, N. and Balch, W. E. (1998). Getting into the Golgi. *Trends Cell Biol.* **8**, 21-25.
Black, V. H. (1972). The development of smooth-surfaced endoplasmic reticulum in adrenal cortical cells of fetal guinea pigs. *Am. J. Anat.* **135**, 381-417.
Bolte, S. and Cordelières, F. P. (2006). A guided tour into subcellular colocalization analysis in light microscopy. *J. Microsc.* **224**, 213-232.
Boschetti, C., Pouchkina-Stantcheva, N., Hoffmann, P. and Tunnacliffe, A. (2011). Foreign genes and novel hydrophilic protein genes participate in the desiccation response of the bdelloid rotifer *Adineta ricciae*. *J. Exp. Biol.* **214**, 59-68.
Browne, J., Tunnacliffe, A. and Burnell, A. (2002). Anhydrobiosis: plant desiccation gene found in a nematode. *Nature* **416**, 38.
Burgess, T. L. and Kelly, R. B. (1987). Constitutive and regulated secretion of proteins. *Annu. Rev. Cell Biol.* **3**, 243-293.
Caprioli, M., Krabbe Katholm, A., Melone, G., Ramløv, H., Ricci, C. and Santo, N. (2004). Trehalose in desiccated rotifers: a comparison between a bdelloid and a monogonont species. *Comp. Biochem. Physiol.* **139A**, 527-532.
Cardenas, J., Rivero, S., Goud, B., Bornens, M. and Rios, R. M. (2009). Golgi localisation of GMAP210 requires two distinct cis-membrane binding mechanisms. *BMC Biol.* **7**, 56-70.
Chakrabarti, A., Chen, A. W. and Varner, J. D. (2011). A review of the mammalian unfolded protein response. *Biotechnol. Bioeng.* **108**, 2777-2793.
Chakrabortee, S., Meersman, F., Kaminski Schierle, G. S., Bertoncini, C. W., McGee, B., Kaminski, C. F. and Tunnacliffe, A. (2010). Catalytic and chaperone-like functions in an intrinsically disordered protein associated with desiccation tolerance. *Proc. Natl. Acad. Sci. USA* **107**, 16084-16089.
Dancourt, J. and Barlowe, C. (2010). Protein sorting receptors in the early secretory pathway. *Annu. Rev. Biochem.* **79**, 777-802.
Dure, L., III, Greenway, S. C. and Galau, G. A. (1981). Developmental biochemistry of cottonseed embryogenesis and germination: changing messenger ribonucleic acid populations as shown by *in vitro* and *in vivo* protein synthesis. *Biochemistry* **20**, 4162-4168.
Dure, L., III, Crouch, M., Harada, J., Ho, T. H. D., Mundy, J., Quatrano, R., Thomas, T. and Sung, Z. R. (1989). Common amino-acid sequence domains among the LEA proteins of higher-plants. *Plant Mol. Biol.* **12**, 475-486.
Emanuelsson, O., Brunak, S., von Heijne, G. and Nielsen, H. (2007). Locating proteins in the cell using TargetP, SignalP and related tools. *Nat. Protoc.* **2**, 953-971.
Furuki, T., Shimizu, T., Kikawada, T., Okuda, T. and Sakurai, M. (2011). Salt effects on the structural and thermodynamic properties of a group 3 LEA protein model peptide. *Biochemistry* **50**, 7093-7103.
Galau, G. A. and Dure, L., III (1981). Developmental biochemistry of cottonseed embryogenesis and germination: changing messenger ribonucleic acid populations as shown by reciprocal heterologous complementary deoxyribonucleic acid-messenger ribonucleic acid hybridization. *Biochemistry* **20**, 4169-4178.
Goyal, K., Tisi, L., Basran, A., Browne, J., Burnell, A., Zurdo, J. and Tunnacliffe, A. (2003). Transition from natively unfolded to folded state induced by desiccation in an anhydrobiotic nematode protein. *J. Biol. Chem.* **278**, 12977-12984.
Goyal, K., Pinelli, C., Maslen, S. L., Rastogi, R. K., Stephens, E. and Tunnacliffe, A. (2005a). Dehydration-regulated processing of late embryogenesis abundant protein in a desiccation-tolerant nematode. *FEBS Lett.* **579**, 4093-4098.
Goyal, K., Walton, L. J. and Tunnacliffe, A. (2005b). LEA proteins prevent protein aggregation due to water stress. *Biochem. J.* **388**, 151-157.

Hammond, C. and Helenius, A. (1995). Quality control in the secretory pathway. *Curr. Opin. Cell Biol.* **7**, 523-529.
Herman, E. M., Tague, B. W., Hoffman, L. M., Kjemtrup, S. E. and Chrispeels, M. J. (1990). Retention of phytohemagglutinin with carboxyterminal tetrapeptide KDEL in the nuclear-envelope and the endoplasmic-reticulum. *Planta* **182**, 305-312.
High, S. (1995). Protein translocation at the membrane of the endoplasmic reticulum. *Prog. Biophys. Mol. Biol.* **63**, 233-250.
Joh, T., Honjoh, K., Yoshimoto, M., Funabashi, J., Miyamoto, T. and Hatano, S. (1995). Molecular cloning and expression of hardening-induced genes in *Chlorella vulgaris* C-27: the most abundant clone encodes a late embryogenesis abundant protein. *Plant Cell Physiol.* **36**, 85-93.
Kikawada, T., Nakahara, Y., Kanamori, Y., Iwata, K. I., Watanabe, M., McGee, B., Tunnacliffe, A. and Okuda, T. (2006). Dehydration-induced expression of LEA proteins in an anhydrobiotic chironomid. *Biochem. Biophys. Res. Commun.* **348**, 56-61.
Lapinski, J. and Tunnacliffe, A. (2003). Anhydrobiosis without trehalose in bdelloid rotifers. *FEBS Lett.* **553**, 387-390.
Letourneur, F., Gaynor, E. C., Hennecke, S., Démollière, C., Duden, R., Emr, S. D., Riezman, H. and Cosson, P. (1994). Coatomer is essential for retrieval of dilysine-tagged proteins to the endoplasmic reticulum. *Cell* **79**, 1199-1207.
Martone, M. E., Zhang, Y., Simpliciano, V. M., Carragher, B. O. and Ellisman, M. H. (1993). Three-dimensional visualization of the smooth endoplasmic reticulum in Purkinje cell dendrites. *J. Neurosci.* **13**, 4636-4646.
McGee, B. (2006). Hydrophilic proteins in the anhydrobiosis of bdelloid rotifers. PhD dissertation, University of Cambridge.
Mundy, J. and Chua, N. H. (1988). Abscisic acid and water-stress induce the expression of a novel rice gene. *EMBO J.* **7**, 2279-2286.
Munro, S. and Pelham, H. R. B. (1987). A C-terminal signal prevents secretion of luminal ER proteins. *Cell* **48**, 899-907.
Pelham, H. R. B. (1990). The retention signal for soluble proteins of the endoplasmic reticulum. *Trends Biochem. Sci.* **15**, 483-486.
Petersen, T. N., Brunak, S., von Heijne, G. and Nielsen, H. (2011). SignalP 4.0: discriminating signal peptides from transmembrane regions. *Nat. Methods* **8**, 785-786.
Popova, A. V., Hundertmark, M., Seckler, R. and Hincha, D. K. (2011). Structural transitions in the intrinsically disordered plant dehydration stress protein LEA7 upon drying are modulated by the presence of membranes. *Biochim. Biophys. Acta* **1808**, 1879-1887.
Pouchkina-Stantcheva, N. N. and Tunnacliffe, A. (2005). Spliced leader RNA-mediated trans-splicing in phylum Rotifera. *Mol. Biol. Evol.* **22**, 1482-1489.
Pouchkina-Stantcheva, N. N., McGee, B. M., Boschetti, C., Tolleter, D., Chakrabortee, S., Popova, A. V., Meersman, F., Macherel, D., Hincha, D. K. and Tunnacliffe, A. (2007). Functional divergence of former alleles in an ancient asexual invertebrate. *Science* **318**, 268-271.
Raykhel, I., Alanen, H., Salo, K., Jurvansuu, J., Nguyen, V. D., Latva-Ranta, M. and Ruddock, L. (2007). A molecular specificity code for the three mammalian KDEL receptors. *J. Cell Biol.* **179**, 1193-1204.
Ricci, C. (1998). Anhydrobiotic capabilities of bdelloid rotifers. *Hydrobiologia* **387**, 321-326.
Sammels, E., Parys, J. B., Missiaen, L., De Smedt, H. and Bultynck, G. (2010). Intracellular Ca^{2+} storage in health and disease: a dynamic equilibrium. *Cell Calcium* **47**, 297-314.
Scriven, D. R. L., Lynch, R. M. and Moore, E. D. W. (2008). Image acquisition for colocalization using optical microscopy. *Am. J. Physiol.* **294**, C1119-C1122.
Segers, H. and Shiel, R. J. (2005). Tale of a sleeping beauty: a new and easily cultured model organism for experimental studies on bdelloid rotifers. *Hydrobiologia* **546**, 141-145.
Shih, M., Hoekstra, F. and Hsing, Y. (2008). Late embryogenesis abundant proteins. *Adv. Bot. Res.* **48**, 211-255.
Sisson, J. K. and Fahrenbach, W. H. (1967). Fine structure of steroidogenic cells of a primate cutaneous organ. *Am. J. Anat.* **121**, 337-367.
Solomon, A., Salomon, R., Paperna, I. and Glazer, I. (2000). Desiccation stress of entomopathogenic nematodes induces the accumulation of a novel heat-stable protein. *Parasitology* **121**, 409-416.
Tolleter, D., Jaquinod, M., Mangavel, C., Passirani, C., Saulnier, P., Manon, S., Teyssier, E., Payet, N., Avelange-Macherel, M. H. and Macherel, D. (2007). Structure and function of a mitochondrial late embryogenesis abundant protein are revealed by desiccation. *Plant Cell* **19**, 1580-1589.
Tolleter, D., Hincha, D. K. and Macherel, D. (2010). A mitochondrial late embryogenesis abundant protein stabilizes model membranes in the dry state. *Biochim. Biophys. Acta* **1798**, 1926-1933.
Tunnacliffe, A. and Lapinski, J. (2003). Resurrecting Van Leeuwenhoek's rotifers: a reappraisal of the role of disaccharides in anhydrobiosis. *Philos. Trans. R. Soc. Lond. B* **358**, 1755-1771.
Tunnacliffe, A. and Wise, M. J. (2007). The continuing conundrum of the LEA proteins. *Naturwissenschaften* **94**, 791-812.
Tunnacliffe, A., Lapinski, J. and McGee, B. (2005). A putative LEA protein, but no trehalose, is present in anhydrobiotic bdelloid rotifers. *Hydrobiologia* **546**, 315-321.
Wiest, D. L., Burkhardt, J. K., Hester, S., Hortsch, M., Meyer, D. I. and Argon, Y. (1990). Membrane biogenesis during B cell differentiation: most endoplasmic reticulum proteins are expressed coordinately. *J. Cell Biol.* **110**, 1501-1511.
Wilson, D. W., Lewis, M. J. and Pelham, H. R. B. (1993). pH-dependent binding of KDEL to its receptor *in vitro*. *J. Biol. Chem.* **268**, 7465-7468.
Wilson, M. R., Yerbury, J. J. and Poon, S. (2008). Potential roles of abundant extracellular chaperones in the control of amyloid formation and toxicity. *Mol. Biosyst.* **4**, 42-52.
Yadav, S., Puri, S. and Linstedt, A. D. (2009). A primary role for Golgi positioning in directed secretion, cell polarity, and wound healing. *Mol. Biol. Cell* **20**, 1728-1736.
Yoshimori, T., Semba, T., Takemoto, H., Akagi, S., Yamamoto, A. and Tashiro, Y. (1990). Protein disulfide-isomerase in rat exocrine pancreatic cells is exported from the endoplasmic reticulum despite possessing the retention signal. *J. Biol. Chem.* **265**, 15984-15990.